Effect of Heat Treatments on the Electrochemical Behavior of 304L Stainless Steel in Nitric Acid

Lingzhen Kong, Kuisheng Wang[*]*, Yupeng Zhan, Yu Zhang*

College of Mechanical and Electrical Engineering, Beijing University of Chemical Technology, Beijing 100029, P.R. China
[*]E-mail: kuishengw@163.com

In this study, the intergranular corrosion behavior of 304L stainless steel (SS) after heating at different temperatures and times was investigated by using the double loop electrochemical potentiokinetic reactivation (DL-EPR), the potentiodynamic polarization electrochemical and the electrochemical impedance spectroscopy (EIS) methods. It was found that there was no significant difference in the potentiodynamic polarization curves of the specimens after different heat treatments. However, the corrosion resistance of specimens could be clearly distinguished by EIS. Between 650 to 750°C, the degree of sensitisation (DOS) had a maximum value and the decrease in R_{ct} was more prominent for the specimens aged at 650 and 750°C. Heat treatments conducted in the range of 650-750°C, even a brief heating time, caused a serious decline in the corrosion resistance of 304L SS. The R_{ct}-values of the specimens aged at 650 and 750°C decreased with the increase of the heating time. However, the R_{ct}-values of the specimens aged at 850°C increased with the increase of the heating time.

1. INTRODUCTION

304L SS, which has excellent corrosion resistance in nitric acid, has been widely used as structural materials for various equipments and pipes handling nitric acid media. However, the hazard of intergranular corrosion is particularly increased during welding procedures. When exposed to concentrated nitric acid, the degradation in corrosion resistance caused by sensitization can seriously affect the lifetime of many industrial components.

Once intergranular corrosion happens, the corrosion resistance and mechanical properties of the 304L SS will become very weak[1]. It is well documented that the intergranular corrosion of austenitic stainless steels is mainly caused by the precipitation of Cr-rich carbides, $M_{23}C_6$, at grain boundaries[2-5]. The diffusivity of Cr in steel is much smaller than that of C. There is not enough chromium added

from grain solid solution to the grain boundary, therefore the forming of Cr-rich carbides only consumes chromium near the grain boundary. Within the matrix adjacent to grain boundaries, there is a Cr-depleted region in which the chromium concentration is less than 12 wt.%[6]. This region, in which the passive film becomes less stable, can be preferentially corroded in concentrated nitric acid.

The $M_{23}C_6$ precipitation process could be divided into three steps, including the diffusion of Cr and C elements to the $M_{23}C_6$/matrix interface, the reaction of Cr and C at the interface, and the growth of $M_{23}C_6$ precipitates[7]. Since the diffusion of Cr is the speed control step of the $M_{23}C_6$ precipitation process, the distribution of the precipitates strongly depends on the sensitizing temperature and exposing period at that temperature. With the sensitization time increasing, there are more Cr-rich carbides precipitated along the grain boundaries. The formation of continuous Cr-depleted region along grain boundaries, which are resulted in by the precipitation of chromium-rich carbides, can lead to serious intergranular corrosion.

The aim of the present investigation was to evaluate the influence of heat treatments on the intergranular corrosion resistance of 304L SS exposed to nitric acid media. The corrosion properties were discussed through the results of the double loop electrochemical potential reactivation (DL-EPR), potentiodynamic polarization and electrochemical impedance spectroscopy (EIS) tests. Optical microscope was utilized to observe the structure and the morphology after electrochemical test of 304L SS.

2. MATERIALS AND METHODS

2.1 Specimen preparation

The specimens of this study were commercial as-rolled 304L SS bar of 10mm diameters. Chemical compositions of the 304L SS used in the present investigation are given in Table 1. A group of specimens were thermally treated at 300°C, 500°C, 600°C, 650°C, 750°C, 850°C, 900°C and 950°C for 15 min, followed by air cooling respectively. Another group of specimens was kept at 650°C, 750°C and 850°C for 5, 15, 30 and 60 min and successively air cooled.

Specially Teflon holder was designed for holding the electrochemical specimens. This Teflon holder could ensure that only the polished surface was exposed to the electrolyte during the electrochemical test. After the heat treatment, the specimens for electrochemical tests were cut into circular cylinder with a height of 6mm by wire-electrode cutting. Then, the specimens were mounted into the Teflon holders as the working electrode.

Before electrochemical tests, the specimens were mechanically polished with SiC emery paper from 400 to 1500 grits size on the working surface. After that, the working surface of the specimen was polished to mirror finish with diamond paste of 3.5 μm particle size. The specimens were ultrasonically rinsed in absolute ethyl alcohol, degreased with acetone, washed with deionized water and dried in a hot air stream.

Table 1. Chemical composition of 304L SS（wt%）.

Alloy	C	Si	Mn	P	S	Ni	Cr	Fe
304L	0.034	0.27	0.62	0.043	0.015	7.904	17.36	Balance

2.2. Electrochemistry measurements

In order to investigate the corrosion resistance of 304L SS specimens subjected to different heat treatments, various electrochemical tests were carried out. A CS350 Electrochemical Workstation was used for electrochemical measurements. The electrochemical corrosion cell employed in this study was made of glass balloon flask with a conventional three electrode system. 304L SS was the working electrode. Ag/AgCl (3.5mol/L KCl) and platinum were used as the reference and the counter electrode respectively. DL-EPR tests were carried out in a 0.5 mol/L H_2SO_4+ 0.01 mol/L KSCN solution at room temperature. The potentiodynamic polarization and EIS tests were conducted in 65 wt.% HNO_3 solution at $40 \pm 1^{\circ}C$.

2.2.1. Double loop electrochemical potentiokinetic reactivation (DL-EPR) tests

The degree of sensitization (DOS) of specimens subjected to different heat treatments was assessed by the DL-EPR test method. When steady state open circuit potential was developed (about 30 min), the DL-EPR tests were initiated. Firstly, the potential sweep from -0.4 V (vs. SSC) in the anodic direction at 0.55 mV/s until the potential reached 0.05 V (vs. SSC). Then the potential was swept back to the initial potential. The chosen reverse potentials, based on the results of cyclic potentiodynamic polarization tests, were located within the stable passive region. The DL-EPR test for each specimen was repeated three times.

The DOS of the heat treated specimens was calculated using the ratio of maximum current density of reactivation (I_r) over maximum current density of activation (I_a) as shown below: DOS = (I_r/I_a) × 100%.

2.2.2. Electrochemical impedance spectroscopy (EIS) measurements

Prior to electrochemical impedance spectroscopy and polarization curve tests, specimens were immersed in the nitric acid solution for 4 hours at open circuit. After measuring open circuit potential, the EIS measurements were conducted at open circuit potential using CS350 Electrochemical Workstation in the frequency range from 0.01 Hz to 100 kHz by superimposing an AC voltage of 10 mV amplitude.

The EIS results could be interpreted by simple "equivalent circuit model" shown in Figure 1. The equivalent circuit description consists of $R_s(CPE_a(R_f(CPE_b||R_{ct})))$ elements was used for fitting and analyzing all the impedance spectral data. In the circuit, R_s was the solution resistance; CPE_a was the interface capacitance of passivation film surface; R_f was the solution resistance within the

corrosion crack; CPE_b was the electric double layer capacitance in parallel connection with R_{ct} which is the charge transfer resistance of corrosion interface. By using Zview Version 3.0 software to fit the EIS data directly, the values of these elements were obtained. The impedance of CPE[8] was given by

$$Z_{CPE} = T[(j\omega)^n]^{-1} \qquad (1)$$

Where T was the proportionality constant; n was the power index value of CPE; ω was the angular frequency and j was the imaginary number equal to $\sqrt{-1}$. T and n were the frequency independent fit parameters. The power index value (n) of CPE was an adjustable fit parameter that lies between 0.5 and 1. For n = 0.5, CPE represents Warburg impedance and n = 1, describes an ideal capacitor[9, 10].
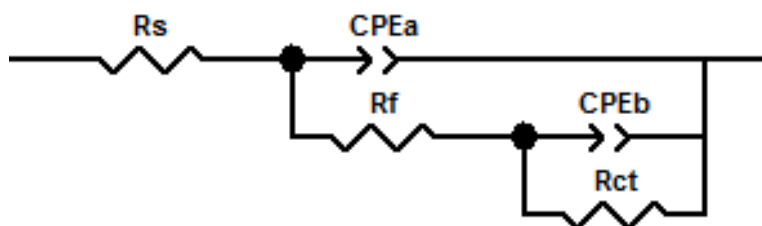
Figure 1. The equivalent circuit model used for fitting the impedance Spectroscopy data.

2.2.3. Potentiodynamic polarization studies

After measuring the open circuit potential and EIS, Potentiodynamic polarization tests were then conducted in a 65 wt.% HNO_3 solution at $40 \pm 1°C$ to study the intergranular corrosion of the specimens. The Ag/AgCl (3mol/L KCl) reference electrode was used to measure the electrode potential of all the mentioned specimens. Potentiodynamic polarization measurements were carried out starting from -100 mV (OCP) to +300 mV (OCP) at a sweep rate of 0.5 mV/s. In order to assess the reproducibility, potentiodynamic polarization measurements were conducted for triplicate specimens in each experimental condition.

The Cview software was used to analyze the potentiodynamic polarization curves. The corrosion parameters, such as corrosion current density (I_{corr}), corrosion potential (E_{corr}), and passivation current density (I_{pass}), were involved in quantitative information which were obtained to comprehend the effect of heat treatments on passivation and corrosion characteristics of 304L SS.

2.3. Microstructure analysis

The corrosion morphology and microstructures of 304L SS were investigated by optical microscopy. The work surface of specimens after the potentiodynamic polarization tests were observed by optical microscopy using a MDS-DM320 microscope.

3. RESULTS AND DISCUSSION

3.1. DL-EPR tests

The results of DL-EPR tests for 304L SS specimens aged at different temperature for 15 min were shown in Figure 2. As the temperature of the heat treatment increased from 0 to 650°C, the sensitization degree of 304L SS became larger. Whereas as the temperature of the heat treatment increased from 750°C to 950°C the sensitization degree became less. Between 650 to 750°C, the value of the sensitization degree of 304L SS raised to the maximum. The degree sensitization of 304L SS increased significantly from 500 to 900°C, which meant that the trend of intergranular corrosion of 304L SS had a specific sensitive temperature range of 500-950°C.

The 304L SS specimens, without heat treatment and at 300°C for 15 min, had the same sensitization degree. When the heat treatment temperature was less than 300°C, the heat treatment of 304L SS would not affect the tendency of the intergranular corrosion. 304L SS was quite susceptible to the sensitization when they were exposed to a high-temperature of 500-850°C[11, 12].
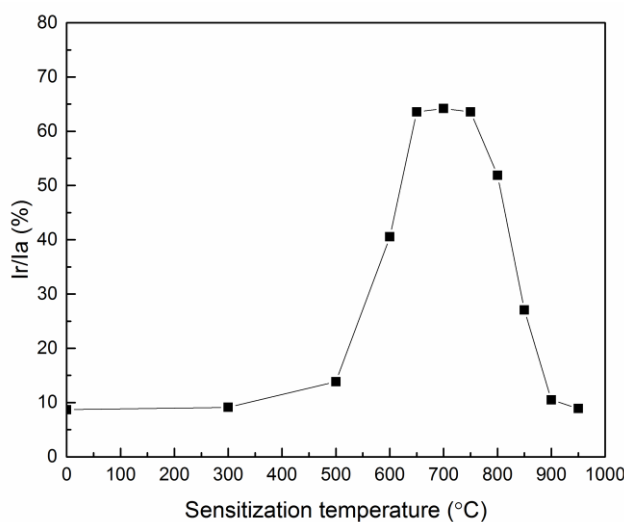
Figure 2. Effect of aged temperature on the I_r/I_a % ratio obtained for the 304L SS aged 15 min at different heat treatment temperature by DL-EPR test in the 0.5 mol/L H_2SO_4+ 0.01 mol/L KSCN solution at room temperature.

The DOS, obtained with DL-EPR tests performed on the 304L SS for heated at 650, 750 and 850°C for various time, was collected in the histogram (see Figure 3). In the temperatures of 650°C and 750°C, with the extension of time of heat preservation, heat treatment of SS intergranular corrosion sensitivity of I_r/I_a showed an increasing trend. When the heat treatment time increased from 5min to 15min, the I_r/I_a % value of the 304L SS specimens heated at 650°C and 750°C increased by 3.5 times and 2.46 times respectively. As the heat treatment time increased from 15 min to 60 min, the DOS value of 304 stainless steel increased slightly, however the susceptibility to intergranular corrosion was very high. In the sensitization temperature range of 650-750°C, 304L SS showed an increased tendency

of DOS as the aging time becoming longer[1]. It was well known that 304L SS was quite susceptible to intergranular sensitization during aging treatment because of precipitation of Cr-rich carbides at grain boundaries[13].

With an increase in heat treatment time from 5 to 60 min, the I_r/I_a % determined for the specimens aged at 850°C decreased. When the aged time was 5 min, the I_r/I_a % ratio increased significantly with the increasing of heating temperature. When the aged time was larger than 15 min, the I_r/I_a % ratio determined for the specimens aged at 650 and 750°C were longer than that determined for the specimens aged at 850°C. These observations supported the hypothesis that there was a thermal activated rediffusion of chromium from the grains inner towards the depleted regions at the heating temperature of 850°C[14].
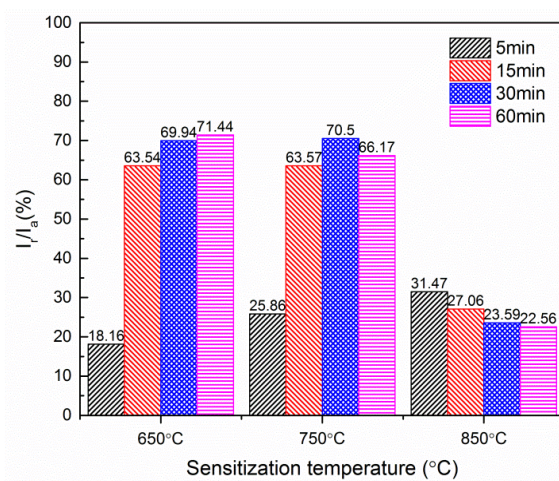
Figure 3. I_r/I_a % determined for the 304L SS aged at 650, 750 and 850°C for various times with DL-EPR tests in the 0.5 mol/L H_2SO_4+ 0.01 mol/L KSCN solution at room temperature.

3.2. Potentiodynamic polarization study
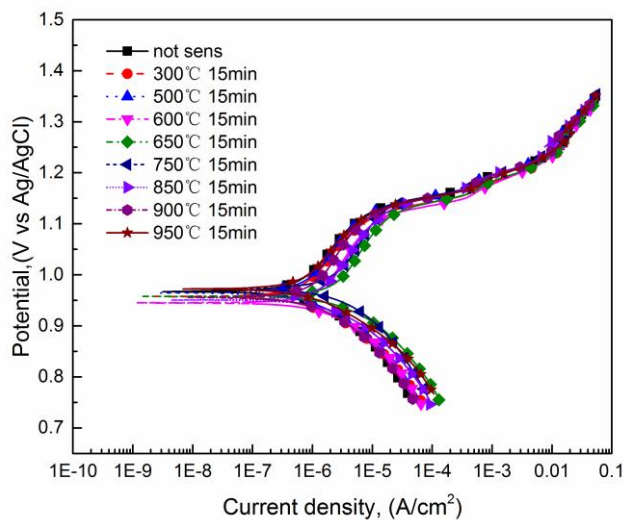
Figure 4. Potentiodynamic polarization plots obtained in 65 wt.% HNO_3 at 40°C for 304L SS aged at different temperature.
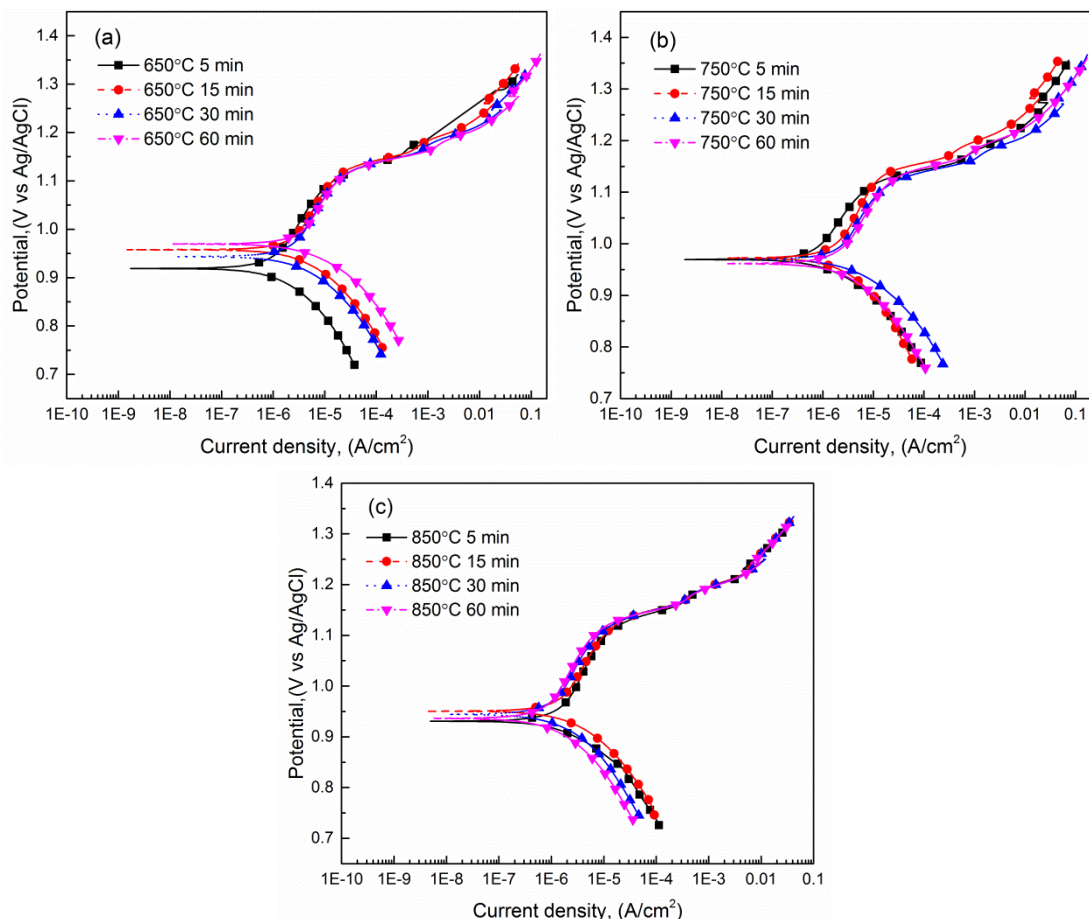
Figure 5. Potentiodynamic polarization plots obtained in 65 wt.% HNO₃ at 40°C for the 304L SS aged at (a) 650, (b) 750 and (c) 850°C for various times.

The potentiodynamic polarization results for all specimens in 65 wt.% HNO₃ are depicted in Figure 4 and Figure 5. The Potentiodynamic polarization curves of 304L SS specimens revealed typical active-passive-transpassive behavior. However, active-passive behaviour was not observed in the polarization plots. After cathodic region, it slowly changed to the passive region followed by transpassive region[15]. It is impossible to distinguish the specimens having different DOS values by their potentiodynamic polarization curves measured in 65 wt.% HNO₃ at 40°C, because all specimens having different DOS values exhibited nearly the same anodic polarization behavior.

The corrosion parameters for 304L SS aged at different temperature were estimated and are mentioned in Table 2. The E_{corr} and I_{corr} values were obtained by the Tafel extrapolation method[9, 16, 17]. The values of the I_{pass} were estimated at a stable passive potential around the middle of the passive region, for all the conditions studied. Compared with other specimens, the high I_{corr} and I_{pass} values obtained in nitric acid solution for 304L SS aged at 650°C and 750°C revealed the worse corrosion resistance. However, no shift in the E_{corr} could be observed for 304L SS aged at different temperature.

The quantitative values for corrosion parameters of 304L SS aged 650°C for various times were calculated and are mentioned in Table 3. With heated time increasing, I_{corr} and I_{pass} for 304L SS aged at 650°C also increased. A similar trend could be observed in the polarization parameters obtained for

304L SS aged at 750°C for various times (Table. 4). However, with heated time increasing, I_{corr} and I_{pass} for 304L SS aged at 850°C decreased (Table. 5). The values of I_{corr} and I_{pass} of 304L SS aged at 650 and 750°C increased for 15 min, 30 min and 60 min, but the values did not change significantly.

It could be concluded from above experimental results that by potentiodynamic polarization curves conducted in 65 wt.% HNO_3 at 40°C could not distinguish the specimens having different DOS.

Table 2. Polarization parameters obtained in 65 wt.% HNO_3 at 40°C for 304L SS aged at different temperature for 15 min.

Temperature °C	b_a /(mV)	b_c /(mV)	I_{corr} /(A/cm^2)	E_{corr} /(V)	I_{pass} /(A/cm^2)
0	249.5	78.716	8.92E-07	0.96711	1.8962E-06
300	223.97	78.595	9.10E-07	0.95746	2.3612E-06
500	215.98	75.922	9.32E-07	0.96444	2.1853E-06
600	289.72	77.875	1.69E-06	0.94502	4.0807E-06
650	397.9	86.82	3.71E-06	0.95772	6.3687E-06
750	341.23	108.9	3.50E-06	0.97242	5.7214E-06
850	249.78	67.299	1.76E-06	0.95058	4.4336E-06
900	236.46	82.231	1.24E-06	0.95549	2.7718E-06
950	201.77	76.697	1.01E-06	0.97247	1.9988E-06

Table 3. Polarization parameters obtained in 65 wt.% HNO_3 at 40°C for 304L SS aged at 650°C for various times.

Heating time min	b_a /(mV)	b_c /(mV)	I_{corr} /(A/cm^2)	E_{corr} /(V)	I_{pass} /(A/cm^2)
5	236.33	104.75	1.45E-06	0.91884	3.19E-06
15	292.87	96.472	3.62E-06	0.95772	6.58E-06
30	305.72	97.448	3.69E-06	0.94333	7.02E-06
60	239.87	64.051	3.92E-06	0.96948	7.61E-06

Table 4. Polarization parameters obtained in 65 wt.% HNO_3 at 40°C for 304L SS aged at 750°C for various times.

Heating time min	b_a /(mV)	b_c /(mV)	I_{corr} /(A/cm^2)	E_{corr} /(V)	I_{pass} /(A/cm^2)
5	251.28	92.759	1.39E-06	0.96968	1.99E-06
15	368.56	142.29	3.51E-06	0.97242	4.30E-06
30	359.88	77.283	3.34E-06	0.96982	4.89E-06
60	319.82	115.67	3.73E-06	0.96149	5.49E-06

Table 5. Polarization parameters obtained in 65 wt.% HNO_3 at 40°C for 304L SS aged at 850°C for various times.

Heating time min	b_a /(mV)	b_c /(mV)	I_{corr} /(A/cm^2)	E_{corr} /(V)	I_{pass} /(A/cm^2)
5	214.66	75.658	1.6154E-06	0.93094	4.1523E-06
15	174.28	57.835	1.4378E-06	0.95058	3.6545E-06
30	170.71	66.992	1.0142E-06	0.9444	2.7069E-06
60	128.98	85.116	8.0095E-07	0.93624	2.2809E-06

3.3 Electrochemical impedance spectroscopy

The electrochemical impedance spectroscopy for 304L SS aged at different temperature for 15min obtained in 65 wt.% HNO_3 at 40°C are presented in Figure 6. The results of EIS test were conducted to elucidate the electrochemical and passive film properties[8, 15, 18]. As observed, all the measured nyquist plots of impedance spectra were characterized by single unfinished semi-circle arc indicating similar corrosion mechanisms. The Nyquist plots (Figure 6) presented a well defined capacitive loop with low frequency impedance limit, which decreased from the specimens aged at 300°C to the specimens aged at 650°C. The impedance arc radius increased gradually by raising the heat treatment temperature from 750°C to 950°C. After aging treatment at 650 and 750°C for 15 min, the impedance arc radius of the specimens were basically the same. the specimens unheated and aged at 300 and 950°C basically had the same value of impedance arc radius. The increase in the semi-circle arc indicated an increase in the film stability and decreasing in semi-circle radius indicates a decrease in the passive film resistance[9, 19].
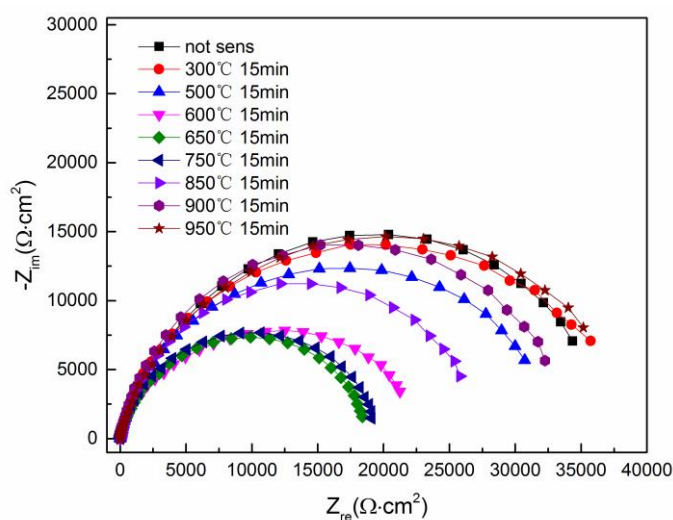
Figure 6. Electrochemical impedance spectroscopy for 304L SS aged at different temperature for 15min obtained in 65 wt.% HNO_3 at 40°C.

The EIS of the 304L SS heated at 650, 750 and 850°C for various times obtained under OCP in 65 wt.% HNO_3 at 40°C are presented in Figure 7(a-c). All the specimens showed only one time constant of an unfinished semi-circle arc. As shown in Figure 7(a), the impedance arc radius decreased with increase in time of heat preservation at 650°C. The specimens aged at 650°C for 30 min and 60 min showed similar and lower semi-circle arc radius compared to the other specimens aged for 5 min and 15 min. The electrochemical impedance spectrum of the specimens aged at 750°C for various times showed a similar trend to that of the correspondent specimens at 650°C. The impedance arc radius of the specimens heated at 850°C increased gradually by increasing the time of heat preservation. The impedance arc radius of the specimens aged for 30 min and 60 min at 850°C were basic coincidence and had higher semi-circle arc radius compared to the other specimens aged for 5 min and 15 min.

The fitted impedance parameters R_S, R_f, CPE_a-T, CPE_a-n, CPE_b-T and CPE_b-n and R_{ct}[20] obtained from Figure 6 are shown in Table 6. The value obtained for R_S was very small when compared to R_{ct} and no specific trend was noticed. The higher R_{ct} value implies good corrosion resistance.
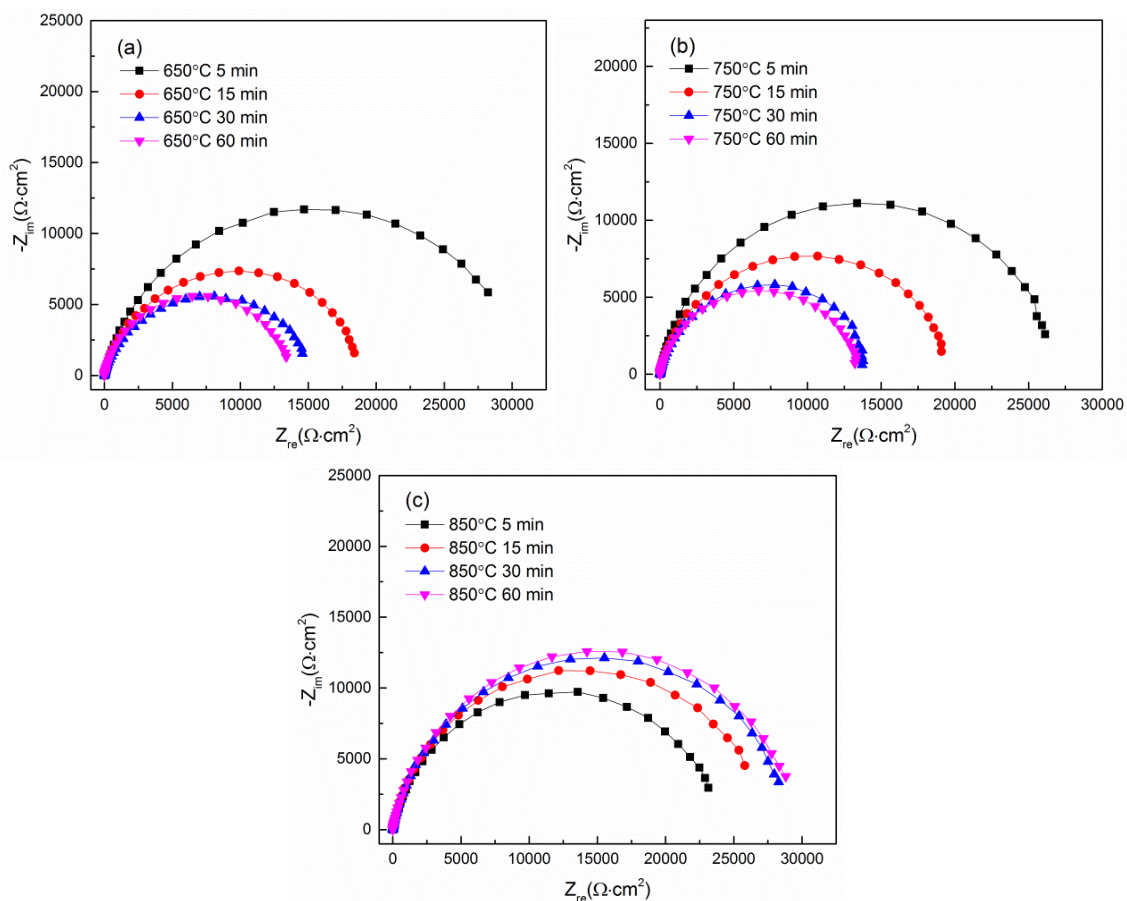
Figure 7. Electrochemical impedance spectrum of the 304L SS aged at (a) 650, (b) 750 and (c) 850°C for various times obtained under OCP in 65 wt.% HNO_3 at 40°C.

Table 6. EIS fitted value of 304L SS aged at different temperature for 15min measured under OCP condition in 65 wt.% HNO_3 at 40°C.

Temperature $^{\circ}$C	R_s /$\Omega \cdot cm^2$	CPE_a-T /$F \cdot cm^{-2}$	CPE_a-n	R_f /$\Omega \cdot cm^2$	CPE_b-T /$F \cdot cm^{-2}$	CPE_b-n	R_{ct} /$\Omega \cdot cm^2$
0	0.62057	3.02E-05	0.92228	3004	2.62E-05	0.67325	36475
300	0.6707	2.97E-05	0.94003	2489.1	2.22E-05	0.5668	31289
500	0.67537	3.38E-05	0.92739	2430.7	2.56E-05	0.64094	30465
600	0.8015	3.82E-05	0.91294	2277	6.07E-05	0.59614	18291
650	0.63717	3.75E-05	0.92366	1903	5.73E-05	0.63878	17829
750	0.66552	3.77E-05	0.92236	2285	6.46E-05	0.64064	17000
850	0.67282	3.16E-05	0.92917	2320	3.01E-05	0.69396	25432
900	0.84102	3.23E-05	0.91918	2899	2.12E-05	0.69401	31790
950	0.64863	3.18E-05	0.92456	2623	2.79E-05	0.61361	39400

The decrease in R_{ct} was more prominent for the specimens heated at 650 and 750°C. The corrosion resistance of 304L SS depended on the spontaneous formation of a protective surface layer[21, 22]. The decrease in the R_{ct} value reflected the reduction of the protective performance of the passive layer. This fact indicated that heat treatments conducted in the temperature range of 650-750°C, even a brief treatment time, could result in a reduction in the corrosion resistance of 304L SS. The R_{ct}-values of the specimens decrease from 36475 $\Omega \cdot cm^2$ to 17829 $\Omega \cdot cm^2$ if the heat treatment temperature was below 650°C, but increase again above 850°C of heat treatment temperature.

The R_{ct}-values of the specimens aged at 650 and 750°C decreased with the increase of the heat treatment time. However, the R_{ct}-values of the specimens aged at 850°C increased with the increase of the heat treatment time. A recovery of the corrosion resistance of the 304L SS was observed for ageing performed at 850°C, this was due to the redistribution of chromium towards the depleted zones[14].

Table 7. EIS fitted value of 304L SS aged at 650°C for various times measured under OCP condition in 65 wt.% HNO_3 at 40°C.

Heating time min	R_s /$\Omega \cdot cm^2$	CPE_a-T /$F \cdot cm^{-2}$	CPE_a-n	R_f /$\Omega \cdot cm^2$	CPE_b-T /$F \cdot cm^{-2}$	CPE_b-n	R_{ct} /$\Omega \cdot cm^2$
5	0.6744	4.24E-05	0.91935	2285	3.05E-05	0.68643	30636
15	0.63717	3.75E-05	0.92366	1903	5.73E-05	0.63878	17829
30	0.62054	3.93E-05	0.91756	1372	4.16E-05	0.61196	14679
60	0.68432	6.98E-05	0.89819	1382	1.18 E-04	0.61541	12180

Table 8. EIS fitted value of 304L SS aged at 750°C for various times measured under OCP condition in 65 wt.% HNO_3 at 40°C.

Heating time min	R_s /$\Omega \cdot cm^2$	CPE_a-T /$F \cdot cm^{-2}$	CPE_a-n	R_f /$\Omega \cdot cm^2$	CPE_b-T /$F \cdot cm^{-2}$	CPE_b-n	R_{ct} /$\Omega \cdot cm^2$
5	0.61732	3.39E-05	0.9317	2441	1.37E-05	0.66269	24788
15	0.66552	3.77E-05	0.92236	2285	6.46E-05	0.64064	17000
30	0.60072	4.64E-05	0.90544	1712	3.01E-05	0.67581	12582
60	0.62531	3.41E-05	0.92915	1433	2.38E-05	0.64715	11449

Table 9. EIS fitted value of 304L SS aged at 850°C for various times measured under OCP condition in 65 wt.% HNO_3 at 40°C.

Heating time min	R_s /$\Omega \cdot cm^2$	CPE_a-T /$F \cdot cm^{-2}$	CPE_a-n	R_f /$\Omega \cdot cm^2$	CPE_b-T /$F \cdot cm^{-2}$	CPE_b-n	R_{ct} /$\Omega \cdot cm^2$
5	0.65841	4.74E-05	0.90854	1175	1.73E-05	0.69361	23449
15	0.67282	4.16E-05	0.92917	2320	1.61E-05	0.69396	25432
30	0.75336	4.15E-05	0.89349	2605	1.32E-05	0.74607	25993
60	0.6019	4.09E-05	0.92028	3279	1.36E-05	0.72438	27151

3.4 Microstructure analysis

Optical microscope images in Figure 8 showed the surface morphology of specimens after the potentiodynamic polarization test in 65 wt.% HNO_3 at 40°C. All the 304L SS specimens displayed grain boundary dissolution, with visibility of well demarcated grain boundaries and a number of shallow and circular pits, in nitric acid solution after the polarization test. Because of intergranular corrosion of 304L SS occurred in nitric acid solution, the corrosion surface of specimens showed considerable damage and high corrugated surface morphology. Deep and narrow grooves were formed along the grain boundaries. For the specimens aged at 650 and 750°C, the corrosion grooves were more pronounced (Figure 8 b and c).

(a)   (b)

(c)   (d)
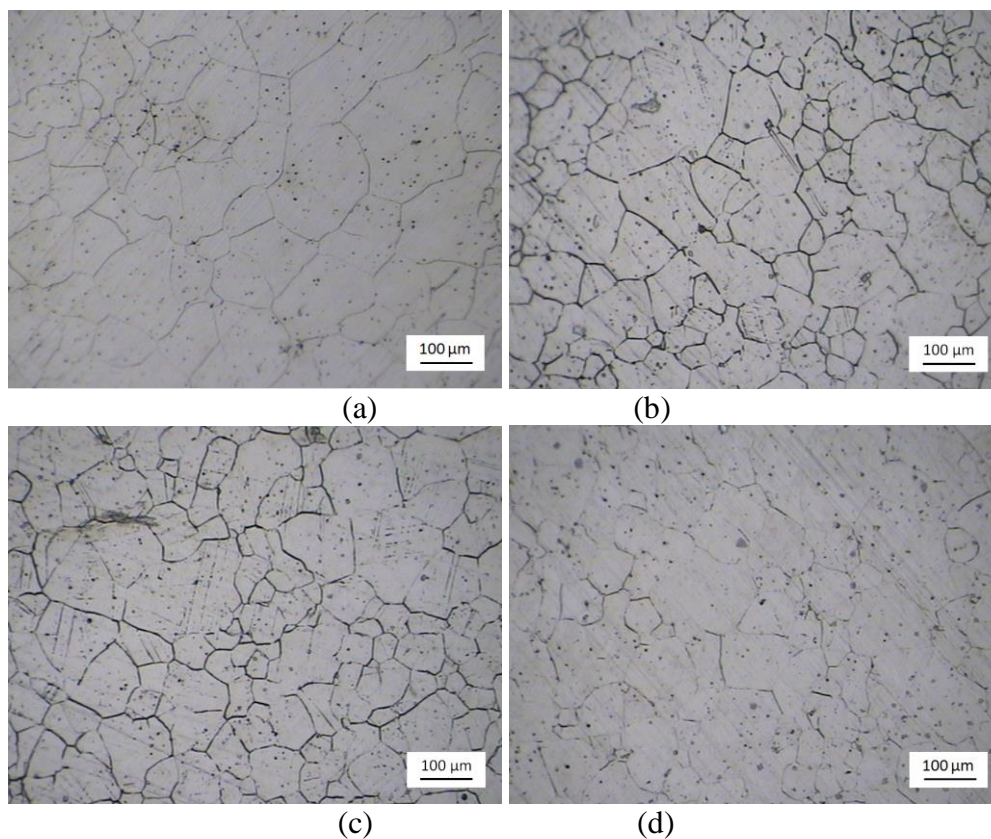
Figure 8. Optical micrographs of 304L SS aged for 15min at (a) 300°C, (b) 650°C, (c) 750°C and (d) 850°C after polarization in 65 wt.% HNO_3 at 40°C.

All grains boundaries are corroded as well as twinning planes. The boundaries of the specimens aged at 850°C were only slightly etched after the polarization test (see Figure 8 d). The corrosion resistance of stainless steels relied on the most effective Cr_2O_3 protective in nitric acid solution[23], and consequently, the impoverishment of chromium in the passive film leaded to the reduction of the corrosion resistance[24]. The chromium-rich chemisorbed film of 304L SS was unstable above transpassive potential in 65 wt.% HNO_3; thus, intergranular attack on the exposed area of 304L SS is induced[6].

4. CONCLUSION

The present research showed the electrochemical properties measured in nitric acid solution for the 304L SS aiming for application in nitric acid unit, such as pipes and holding vessels.

1.   Brief heat treatments, carried out in the temperature range of 500-900°C, resulted in a significant increase in the DOS of 304L SS. Between 650 to 750°C, the DOS of 304L SS had a maximum value.

2.   The result of EIS test showed that, the decrease in R_{ct} was more prominent for the specimens aged at 650 and 750°C. The R_{ct}-values of the specimens aged at 650 and 750°C declined with the increase of the heat treatment time. However, the R_{ct}-values of the specimens aged at 850°C increased with the increase of the heat treatment time.

3.   By potentiodynamic polarization curves, we could not distinguish the 304L SS with the differences in heat treatment. However, the corrosion resistance of 304L SS could be clearly distinguished by the EIS. The EIS test results were virtually in agreement with DL-EPR test results.

4.   All the 304L SS specimens displayed grain boundary dissolution, with visibility of well demarcated grain boundaries and a number of shallow and circular pits, in nitric acid medium after the polarization test. For the specimens aged at 650 and 750°C, the corrosion grooves along the grain boundaries were more prominent. The boundaries of the specimens aged at 850°C were only slightly etched after the polarization test.

References

1. J. Jiang, D. Xu, T. Xi, M.B. Shahzad, M.S. Khan, J. Zhao, X. Fan, C. Yang, T. Gu and K. Yang, *Corros. Sci.*, 113 (2016) 46.
2. J.K. Kim, Y.H. Kim, B.H. Lee and K.Y. Kim, *Electrochim. Acta*, 56 (2011) 1701.
3. H. Sahlaoui, K. Makhlouf, H. Sidhom and J. Philibert, *Mater. Sci. Eng., A*, 372 (2004) 98.
4. M. Terada, M. Saiki, I. Costa and A.F. Padilha, *J. Nucl. Mater.*, 358 (2006) 40.
5. A.Y. Kina, V.M. Souza, S.S.M. Tavares, J.A. Souza and H.F.G. de Abreu, *J. Mater. Process. Technol.*, 199 (2008) 391.
6. C.-A. Huang, Y.-Z. Chang and S.C. Chen, *Corros. Sci.*, 46 (2004) 1501.
7. J. Qian, C. Chen, H. Yu, F. Liu, H. Yang and Z. Zhang, *Corros. Sci.*, 111 (2016) 352.
8. S. Ningshen, U. Kamachi Mudali, G. Amarendra and B. Raj, *Corros. Sci.*, 51 (2009) 322.
9. S. Ningshen, U. Kamachi Mudali, S. Ramya and B. Raj, *Corros. Sci.*, 53 (2011) 64.
10. J. Jayaraj, A. Ravi Shankar and U. Kamachi Mudali, *Electrochim. Acta*, 85 (2012) 210.

11. A. Pardo, M.C. Merino, A.E. Coy, F. Viejo, M. Carboneras and R. Arrabal, *Acta Mater.*, 55 (2007) 2239.
12. A. Arutunow and K. Darowicki, *Electrochim. Acta*, 53 (2008) 4387.
13. K. Kaneko, T. Fukunaga, K. Yamada, N. Nakada, M. Kikuchi, Z. Saghi, J.S. Barnard and P.A. Midgley, *Scripta Mater.*, 65 (2011) 509.
14. F. Zanotto, V. Grassi, M. Merlin, A. Balbo and F. Zucchi, *Corros. Sci.*, 94 (2015) 38.
15. N. Padhy, S. Ningshen, B.K. Panigrahi and U. Kamachi Mudali, *Corros. Sci.*, 52 (2010) 104.
16. J.R. Galvele, *Corros. Sci.*, 47 (2005) 3053.
17. F. Mansfeld, *Corros. Sci.,* 47 (2005) 3178.
18. M. Saadawy, *Int. J. Electrochem. Sci.,* 11 (2016) 2345.
19. M. Terada, D.M. Escriba, I. Costa, E. Materna-Morris and A.F. Padilha, *Mater. Charact.*, 59 (2008) 663.
20. Y.J. Si, Z.P. Xiong, X.W. Zheng, M.J. Li and Q.H. Yang, *Int. J. Electrochem. Sci.*, 11 (2016) 3261.
21. N. Padhy, R. Paul, U. Kamachi Mudali and B. Raj, *Appl. Surf. Sci.*, 257 (2011) 5088.
22. L. Jinlong, L. Hongyun, *Appl. Surf. Sci.,* 263 (2012) 29.
23. P. Fauvet, F. Balbaud, R. Robin, Q.T. Tran, A. Mugnier and D. Espinoux, *J. Nucl. Mater.*, 375 (2008) 52.
24. R. Robin, F. Miserque and V. Spagnol, *J. Nucl. Mater.*, 375 (2008) 65.